Effects of Decalage on Distributed Lift Configurations

Michael Mongin[1] and Andrew Truszkowski[1]

Aaron Altman[2]

University of Dayton, Dayton, Ohio, 45469

Abstract

Previous experimental and numerical studies showed that an unoptimized array of mini wings tested at a Reynolds number on the order of 10,000 to 30,000 yielded 60 to 70 percent of the aerodynamic efficiency achieved by a mono wing of the same aspect ratio and reference area [1]. Building on those results, this study will further analyze the effect of decalage variation of downstream wings in the two row, multi column configuration in order to seek a higher efficiency than previously found. The present study will be performed first numerically using vortex lattice method codes and then experimentally in a low speed wind tunnel in order to validate the vortex lattice method analysis and better understand the dependence on viscous effects of this geometry change on the wing sets. The results from the decalage study will be used to analyze the system level impact of these configuration sensitivities through Breguet Range. The results will then be compared to previous suboptimal multi-wing configurations as well as a current conventional mono wing baseline similar to that found on existing aircraft.

NOTE TO REVIEWERS: Both the parametric numerical study and the experimental investigation are continuing this summer and a more complete set of results will be presented in the final paper [if accepted]. In particular, VLM data for a wider range of cambered multi-wing sets and force based wind tunnel data of select configurations as informed from the VLM study.

I. Introduction

The distributed lift configuration that utilizes multi-wing sets to generate equal or comparable lift and aerodynamic efficiency to a mono wing configuration of equal wing area and aspect ratio is the goal of this research. These configurations would place small wings on the order of 6 to 12 per side; into a grid like arrangement with rows and columns to disperse the lift longitudinally along the aircraft. Keeping the aspect ratio and total reference area the same between the mini wing and the mono wing configurations allow for a direct comparison of the lift and drag coefficients without compromising critical variables that affect the final value, save for the difference in Reynolds number across a mini wing configuration when compared to the mono-wing. In this range of Reynolds numbers, it is believed that the penalty of the lower Reynolds number flow over the mini wing set will aide in establishing a conservative margin that at higher Reynolds numbers will have a diminished deficit between multi-wing and mono wing cases due to reduced boundary layer effect . The benefits of a configuration utilizing multiple miniature wings over larger single wings are as follows:

- Conventionally configured aircraft wings are one of the heaviest components of the airplane structure.
- They are costly and difficult to manufacture, transport, and install on aircraft due to their sheer size and complexity.
- Additionally, at airport terminals, much of the space that airplanes occupy results directly from their large wingspans. Since aerodynamic lift is a strong function of the wing planform surface area, the size of the wing planform is determined based on the amount of lift desired (or weight to offset).
- These mini wings can be easily and inexpensively mass produced.
- They can be produced with higher effective aspect ratios than the monoplane wing.
- They can be manufactured considerably lighter. [2]
- Maneuverability would be improved due to reduced inertia and the potential for additional control from having control surfaces distributed across numerous miniature wings.

[1] Undergraduate Student, Mechanical and Aerospace Department, AIAA Member. monginm1@udayton.edu
[2] Tech Advisor, United States Air Force Research Laboratory, AFRL/RQVA, AIAA Associate Fellow, aaron.altman.1@us.af.mil

- Damage tolerance would also be improved as an airplane could afford to lose many wings before suffering large losses in lift.
- Additionally, the wake shed from the aircraft would be an order of magnitude more compact, and of course the overall size of the vehicle would be much more compact than a standard monoplane wing.

Previous experimental work on this concept has shown that the aerodynamics of these configurations are feasible for reaching lift over drag performance on the order of 60 to 70 percent that of a mono wing configuration of equal wing area and aspect ratio [1]. These results were found with models that were based on pure gap and stagger variation and did not take into account any other geometry or spacing parameterization. The goal of the present study is to better understand the effects of changing the angle of attack in the streamwise direction of a set of wings. Figure 1 shows the variation of these wing sets in a single row, multi column configuration with Figure 1a being the 6 degrees angle of attack variation and Figure 1b being a standard 0-degree angle of attack variation.

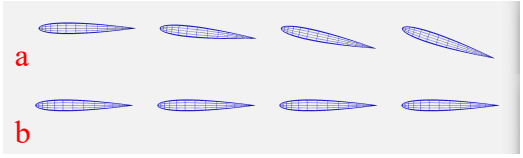

Figure 1. Downstream Change in Angle of Attack VLM Models

The present study will begin with a numerical Vortex Lattice Method VLM analysis on the change in downstream wings angle of attack in order to determine the best aerodynamic case for creating physical models to be wind tunnel tested. Multiple wing sets variations will be tested in the VLM code to better understand the numerically predicted effects of the changes in angle of attack of downstream wings. Leveraging knowledge from biplane studies from Kang and Genco [3], optimal gap placement and decalage angle of wings in the multi-wing set were determined. With information from Mongin and Truszkowski [1], optimal stagger and number of streamwise wings was determined. Once these baselines are set, sensitivities on the angle of wings downstream relative to fixed lower wing rows will be conducted. The best cases from these initial tests will be taken and rapid prototyped for wind tunnel testing to verify their performance and the applicability of the VLM code for these types of configurations.

In order to quantify the impact that a change in the lift to drag ratio has on an air vehicle, analysis is done using the Breguet Range Equation to arrive at the effective range of the vehicle with supplemental consideration of the change in weight due to the reduced mass of the wings and the decrease in aerodynamic efficiency due to the implementation of the multi-wing configuration on 3 standard aircraft, the Cessna 172, a Boeing F-18E, and a Boeing 747-100. This analysis was previously performed by Mongin and Truszkowski [1] on the standard wing configurations with sensitivity on gap and stagger and the results from this study will be compared with those as well.

II. Previous Research

Previous studies were leveraged to provide context for the present research [2]. One study compared the effects of gap (vertical spacing between wings) and stagger (horizontal spacing between wings) on lift. Gap and stagger can be seen in Figure 2 below. In terms of gap, the smaller the gap, the smaller the downwash angle coming off the trailing edge of the wing. A smaller downwash angle implies less lift. Figure 3, below, provides an example.

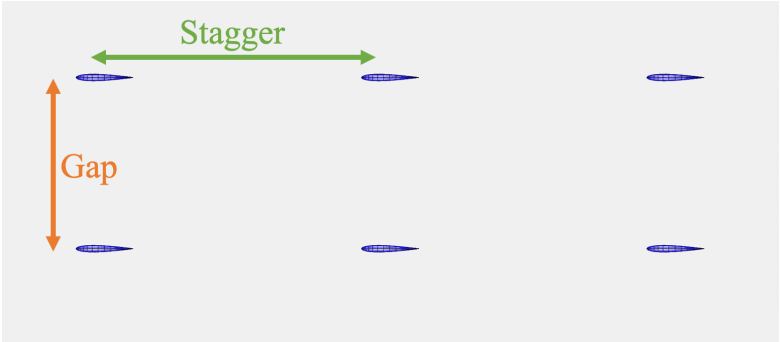

Figure 2. Gap and Stagger Visualization

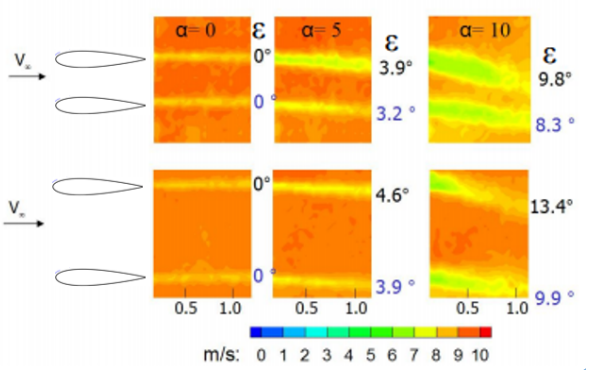

Figure 3. Effect of Gap on Lift (half and one-chord gaps shown)

The two comparisons depicted above in Figure 3 show two wings with a 0.5 chord length gap and a 1.0 chord length gap respectively. Clearly, the 1.0 chord length gap shows larger downwash angles on both of the wings, with the top wing generating the most lift in both cases. The present study did not explicitly study gap, the focus was on stagger first. In the previous study, it was also determined that the coefficient of lift decreased as the stagger decreased when the stagger was less than 1.0 chord length. An interesting conclusion from that study, however, was that beyond a stagger of about 1.2 chord lengths, the amount of lift gained as stagger increases is negligible, the lift tapers off at a certain value and the lift is no longer significantly affected by the stagger. Figure 4 shows the results from previously published simulations. These results informed rational starting points for gap and stagger necessary to minimize lifting surface interactions. This valuable information was applied to the studies described in the upcoming sections.

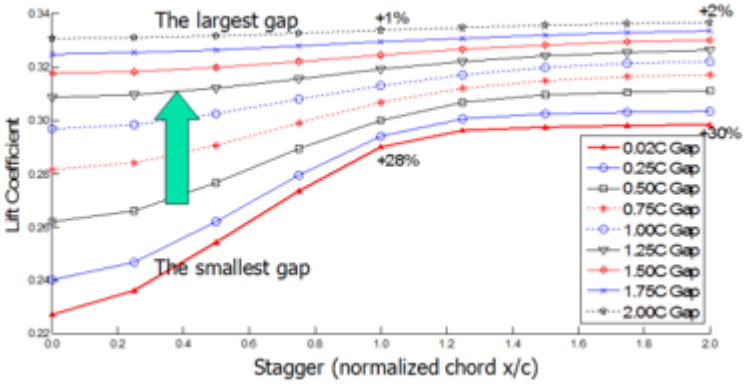

Figure 4. Effects of Stagger and Gap on Lift

Another previous study by Mongin and Truszkowski showed that simplified multi-wing sets arranged in two row multicolumn configurations as seen below in Figure 5, could generate 60 to 70 percent of the aerodynamic efficiency of an equivalent mono wing while keeping overall system sizing in mind. The sets tested in this study were NACA0012 airfoils with a chord length of 1.47 cm and 5.8 cm semi span. A baseline NACA0012 was also used with a semi span aspect ratio of 4 and equal reference area to the multi-wing sets. The wings in this study were kept at 0 degrees incidence relative to one another and the vertical wing orientation in the sets at 0 stagger. Variation of the spacing vertically (gap) and horizontally (stagger) was performed to find an optimum wing spacing that yielded comparable results to a mono wing without increasing the sizing of the system drastically. The wind tunnel results of this study are shown in Figure 6 where it can be seen that the wing set that implemented 3 chord lengths of vertical spacing and 4 chord lengths of horizontal spacing yielded the highest aerodynamic efficiency of the cases tested.

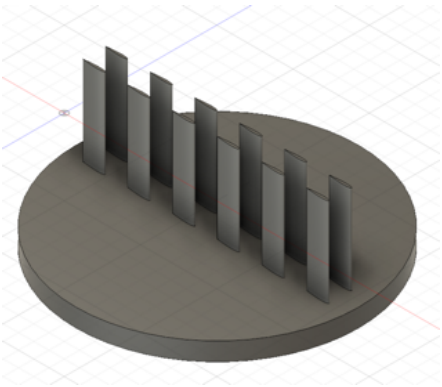

Figure 5. Multi wing set example

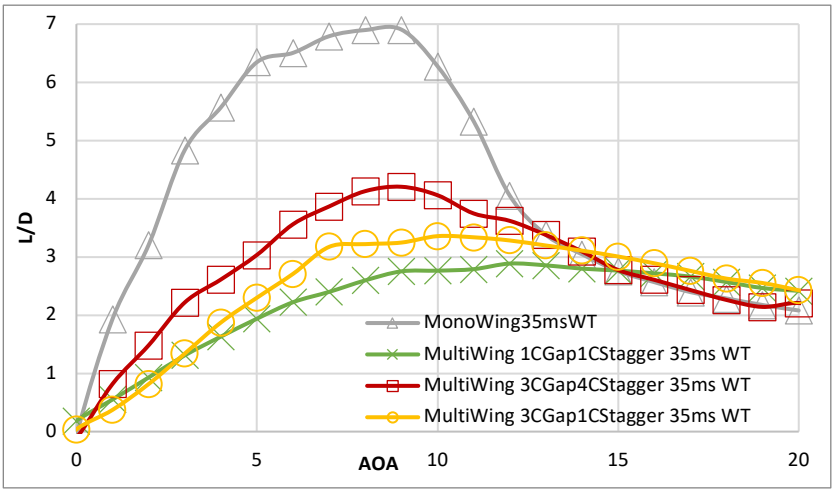

Figure 6. Multi wing wind tunnel results

III. Experimental and Numerical Background

The previous studies results were leveraged for the creation of a test matrix to be run in the numerical portion of this study. The aim of the numerical investigation is to find configurations where Vortex Lattice Method (VLM) codes predict there will be higher aerodynamic efficiency in order to limit the need for excessive experimental testing. Once the numerical tests are run and the appropriate configurations are chosen, the experimental tests will be conducted to determine the force-based testing results of the aerodynamic efficiencies of the different test sets. A known issue with this method is the inability for the VLM codes to model the parasitic drag of the wings accurately. This was noted in the previous work by Mongin and Truszkowski where the OpenVSP models executed through VSPAero were compared to the wind tunnel tests and the parasitic drag of the VLM results were removed due to their inaccuracies. The lift induced drag of the VLM results was used however and by using the wind tunnel data, a 0 angle of attack (no lift) drag value was extracted and used as a base drag offset for the VLM results. The results of this approach are shown below in Figure 7 along with the wind tunnel data for comparison. At lower angles of attack the lift induced drag predictions of the VLM calculations are very close to the wind tunnel results.

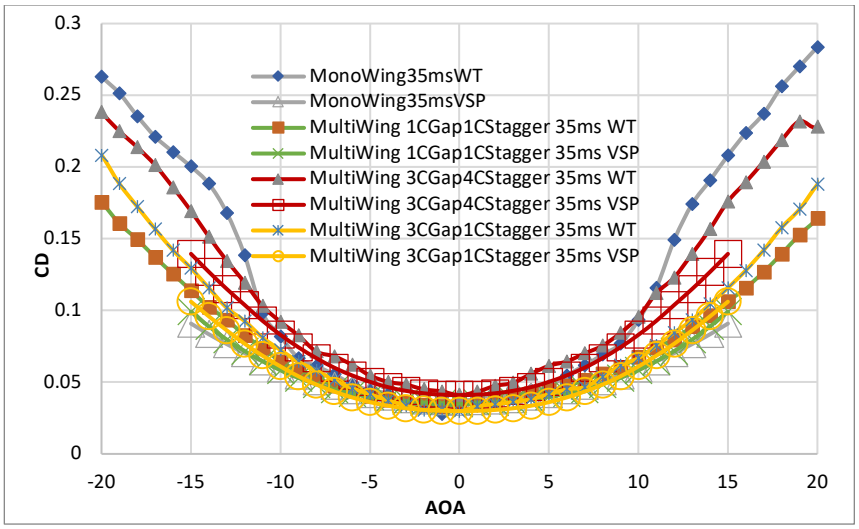

Figure 7. VLM data with offset drag from wind tunnel results

A. Experimental Setup

The experimental investigation was conducted at the University of Dayton Low-Speed Wind Tunnel (UD-LSWT). A photo of the tunnel is shown below in Figure 8. The UD-LSWT has a 16:1 contraction ratio, 6 anti-turbulence screens and 4 interchangeable 76.2 cm x 76.2 cm x 243.8 cm (30" x 30" x 96") test sections. The test section is convertible from a closed jet configuration to an open jet configuration with the freestream range of 6.7 m/s (20 m/s) to 40 m/s (140 ft/s) at a freestream turbulence intensity below 0.1% measured by hot-wire anemometer. The tunnel can also vary the freestream velocity profile at up to 5 Hz and over 50% velocity amplitude using a downstream shuttering system.

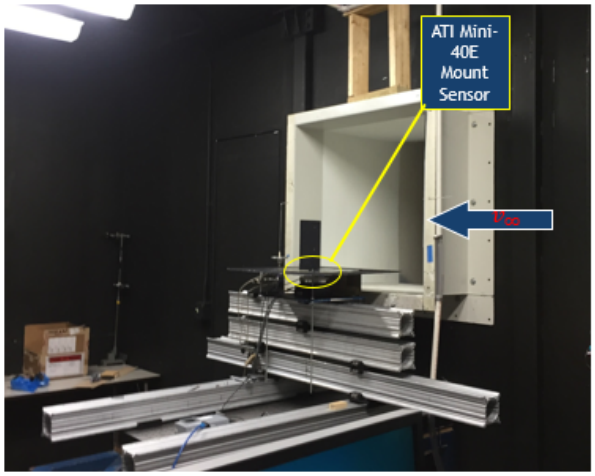

Figure 8. University of Dayton Low-Speed Wind Tunnel

The experiments were performed in the open jet configuration where an inlet of 76.2 cm x 76.2 cm opens to a pressure sealed plenum. Figure 3.1 shows the experimental setup. The effective length of the test section in the open jet configuration is 182 cm. A 137 cm x 137 cm collector collects the expanded jet on its return to the diffuser. The velocity variation for a given RPM of the wind tunnel fan is found using a Pitot-static tube connected to an TSI differential pressure transducer (Range: 0 – 6.9 kPa).

An ATI Industrial Automation Mini-40 sensor was used to measure the normal (N) and axial (A) forces. The specifications for the Mini – 40 sensor are as follows: the normal and axial forces were measured using the X and Y axis of the sensor with magnitude ranges of 40 N and a resolution of 1/100 N, while the torque ranges of the X and Y axes were 2 Nm with resolutions of 1/4000 Nm. The sampling rate during data acquisition from the Mini-40 was 100 Hz. Wind-off tare values were taken before and after each test, and then the normal and axial force readings were

adjusted for any drift that may have occurred. Lift and drag forces could be calculated from the normal and axial forces using the following equations below.

$$L = N\cos\alpha - A\sin\alpha \quad (1)$$
$$D = N\sin\alpha + A\cos\alpha \quad (2)$$

The test models themselves will be 3D printed on a Stratasys uPrint SE Plus printer at the University of Dayton Maker Space. The models will consist of a circular plate of 185 mm diameter and 12 mm thickness. The wings will be printed directly to the plate and an interface to mount the plate to the mini-40 sensor was constructed. An image of the CAD model of the test model is shown below in Figure 9.

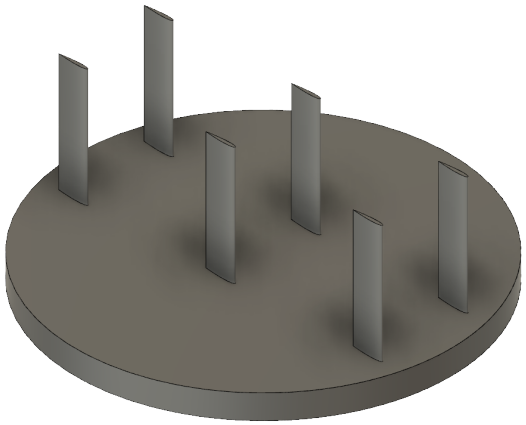

Figure 9. Baseline test case of multi-wing configuration

B. Numerical Background

VSPAERO was used to study the effects of lift and [inviscid] drag resulting from variations in gap, stagger, span and relative mini-wing angle of attack. This tool is an extension of the OpenVSP software which was released for public use by NASA in 2012. The software is centered on air vehicle design and allows for parameterization of a wide range of design inputs. This made application of OpenVSP to this project natural due to its versatility in modifying geometry. As seen in Figure 10, the interface for modifying wing location of the set was well designed and made changing the locations straightforward. The vortex lattice method code included with OpenVSP, VSPAERO, made batch processing of each wing set evident as well. VSPAERO allows the user to specify the angle of attack, angle of sideslip, and Mach number ranges for a specific geometry test set in the flow conditions input section of the dialog box. It also allows manual control of the wing area, chord, and span used for the Vortex Lattice Method (VLM) calculations. This manual control is important for these studies as many VLM codes don't use the area from the system of wings as a reference area and assume a single wing area as the Sref. In addition, the process to read and process the output file from VSPAERO is effortless. The user is provided with a document in a comma separated value format that includes coefficient of lift, coefficient of induced drag, coefficient of parasitic drag, and lift over drag for each parameter specified in the flow condition input section. This format is simple to parse in Microsoft Excel and affords a rapid turnaround executing a test and combining the results next to data from multiple sources for subsequent plotting. The VSP environment enabled the discovery of relationships as a function of each parameter change made and helped in deciding which ones to investigate further through experimental study.

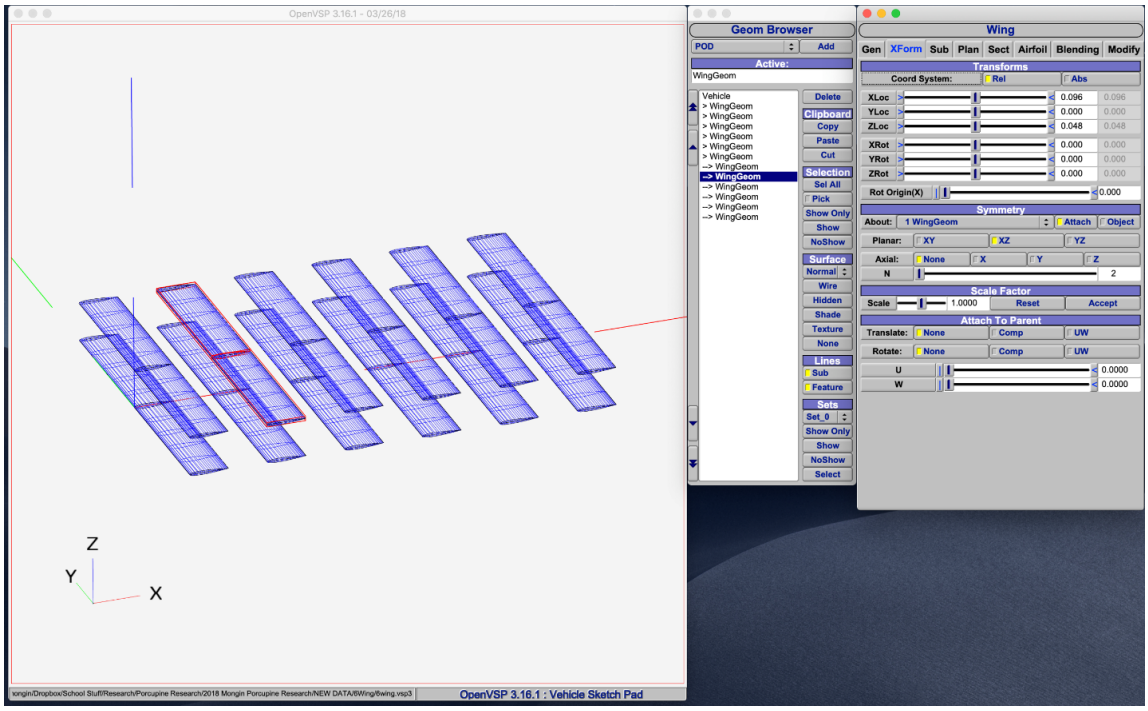

Figure 10. Shows the OpenVSP Rendering screen as well as the input dialog box interface for a 12-wing, 1 chord gap, 1 chord stagger case.

IV. Experimental and Numerical Investigations

A. Numerical Investigation

The numerical investigation of this study begins with the findings of the Mongin and Truszkowski study which concluded that a multi-wing configuration of 2 rows of wings with 3 columns staggered at 4 chord lengths with a 3 chord gap yielded the best aerodynamic efficiency when considering the volume of the configuration. This 3 chord gap, 4 chord stagger configuration was the starting point of the numerical test matrix and iterations to this initial model were made in order to study the effects of changing the angle of attack of the wings downstream with both fixed lower wings at 0 angle of attack and lower wings following the same angle of the upper wing in the set. The stagger of the top wing with respect to the column will also be taken into account in 1 chord length intervals from -1 to 1 in order to implement the Knag and Genco findings on the effects of stagger of the wings vertically. An example of the upper wing stagger and downstream angle of attack is shown below in Figure 11. Each of these models will be tested at 15 and 30 meters per second (m/s) for sensitivity of the configurations to different Reynolds numbers and from -40 to 40 degrees angle of attack. The larger range of angle of attack is needed to fully develop the stall of the wing sets as found by Mongin and Truszkowski in a previous study on these multi-wing sets. The test matrix is shown below in Table 1 and includes 150 individual cases. The best aerodynamic efficiency sets from this study will be used to down select for the experimental testing. Results and discussion from the numerical study will be displayed here once completed. The relevance for the sets chosen to move forward with for experimentation will also be explained.

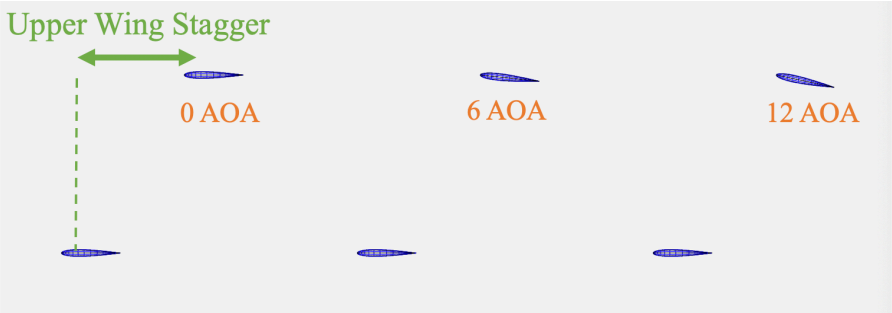

Figure 11. Upper wing stagger and change in angle of attack downstream (6 degrees)

Table 1: Numerical Test Matrix

Bottom Row Delta Alpha	Top Row Delta Alpha	Top Row Stagger	Free Stream	System Angle of Attack
0 Degrees	0 Degrees	-1C, 0C, 1C	15 and 30 m/s	-40 to 40 Degrees
0 Degrees	1 Degrees	-1C, 0C, 1C	15 and 30 m/s	-40 to 40 Degrees
0 Degrees	2 Degrees	-1C, 0C, 1C	15 and 30 m/s	-40 to 40 Degrees
0 Degrees	3 Degrees	-1C, 0C, 1C	15 and 30 m/s	-40 to 40 Degrees
0 Degrees	4 Degrees	-1C, 0C, 1C	15 and 30 m/s	-40 to 40 Degrees
0 Degrees	5 Degrees	-1C, 0C, 1C	15 and 30 m/s	-40 to 40 Degrees
0 Degrees	6 Degrees	-1C, 0C, 1C	15 and 30 m/s	-40 to 40 Degrees
0 Degrees	7 Degrees	-1C, 0C, 1C	15 and 30 m/s	-40 to 40 Degrees
0 Degrees	8 Degrees	-1C, 0C, 1C	15 and 30 m/s	-40 to 40 Degrees
0 Degrees	9 Degrees	-1C, 0C, 1C	15 and 30 m/s	-40 to 40 Degrees
0 Degrees	10 Degrees	-1C, 0C, 1C	15 and 30 m/s	-40 to 40 Degrees
0 Degrees	11 Degrees	-1C, 0C, 1C	15 and 30 m/s	-40 to 40 Degrees
0 Degrees	12 Degrees	-1C, 0C, 1C	15 and 30 m/s	-40 to 40 Degrees
1 Degrees	1 Degrees	-1C, 0C, 1C	15 and 30 m/s	-40 to 40 Degrees
2 Degrees	2 Degrees	-1C, 0C, 1C	15 and 30 m/s	-40 to 40 Degrees
3 Degrees	3 Degrees	-1C, 0C, 1C	15 and 30 m/s	-40 to 40 Degrees
4 Degrees	4 Degrees	-1C, 0C, 1C	15 and 30 m/s	-40 to 40 Degrees
5 Degrees	5 Degrees	-1C, 0C, 1C	15 and 30 m/s	-40 to 40 Degrees
6 Degrees	6 Degrees	-1C, 0C, 1C	15 and 30 m/s	-40 to 40 Degrees
7 Degrees	7 Degrees	-1C, 0C, 1C	15 and 30 m/s	-40 to 40 Degrees
8 Degrees	8 Degrees	-1C, 0C, 1C	15 and 30 m/s	-40 to 40 Degrees
9 Degrees	9 Degrees	-1C, 0C, 1C	15 and 30 m/s	-40 to 40 Degrees
10 Degrees	10 Degrees	-1C, 0C, 1C	15 and 30 m/s	-40 to 40 Degrees
11 Degrees	11 Degrees	-1C, 0C, 1C	15 and 30 m/s	-40 to 40 Degrees
12 Degrees	12 Degrees	-1C, 0C, 1C	15 and 30 m/s	-40 to 40 Degrees

B. Experimental Investigation

The experimental results of this study will be included here along with a discussion about their findings. It is expected that the drag results will again be lower due to the inability of the VLM code to model the parasitic drag properly. It is expected that the new sets will exhibit slightly higher coefficient of lift due to the shift in upper row stagger and angle of attack. As in the previous work on these configurations [1] the aerodynamic efficiency will be displayed after a breakdown of the coefficient of lift and drag results directly. The aerodynamic efficiency will then be used in the following section for analysis. A finding of Mongin and Truszkowski [1] that will also be analyzed here is the stall angle for the sets which was previously found to be in the range of 35 degrees angle of attack. Comparisons with previous wind tunnel data from Mongin and Truszkowski will also be made.

Although no testing has been done for the present study, the exact experimental setup was used for a previous study and the results from the present will be compared to the previous results once completed. Included below in Figures 12 and 13 are the plots of the wind tunnel data taken from the previous research on this topic.

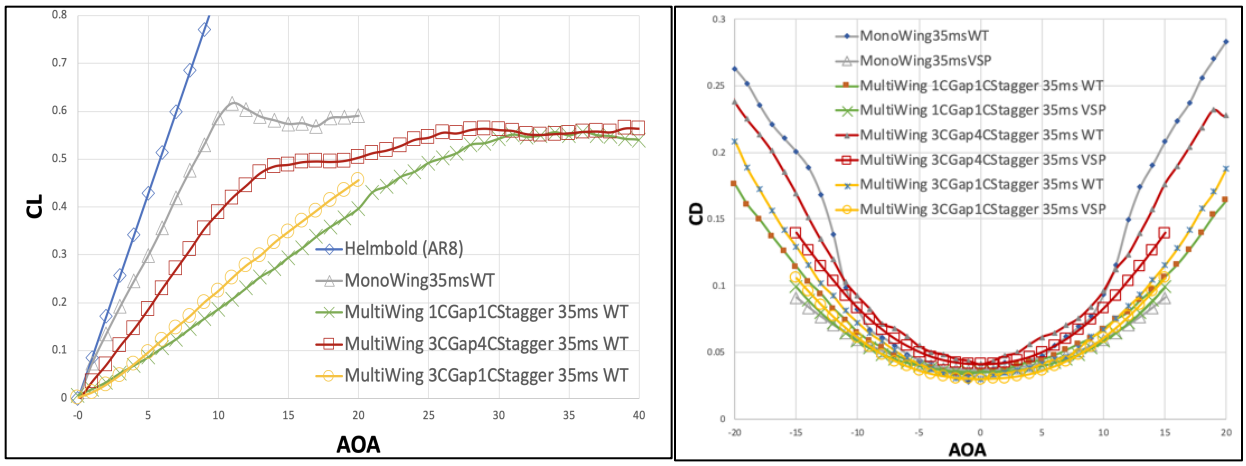

Figure 12. Coefficient of lift (Wind Tunnel) and coefficient of drag (Wind Tunnel and VLM)

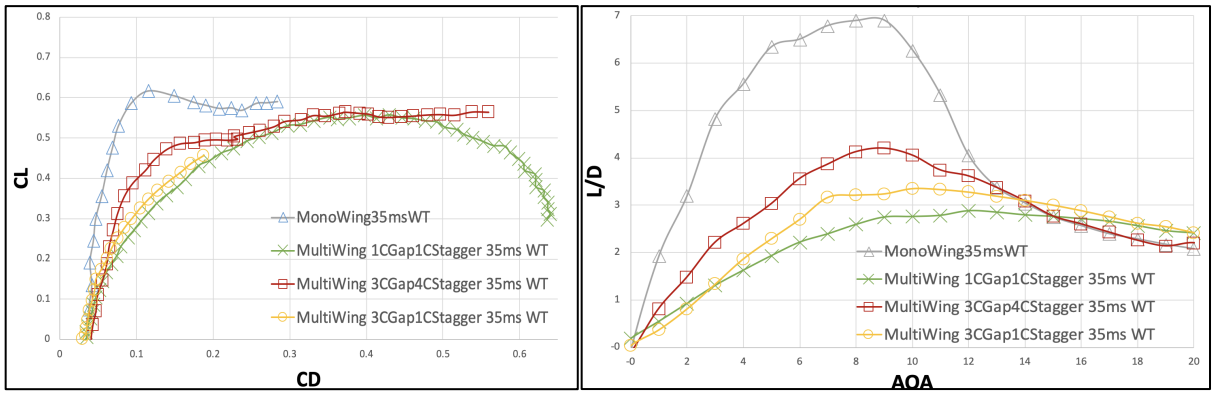

Figure 13. Drag polar and aerodynamic efficiency (Wind Tunnel)

V. System-Level Impacts

A. System-Level Impacts

The next part of this study looked at a real-world application of distributed lift configurations. As mentioned in the introduction, there are a number of benefits that distributed lift configurations would have over the conventional mono-wing aircraft, with the drastic reduction in wing weight being the most useful. Standard large commercial airliners have wing densities of roughly 9 pounds per square foot, per Raymer [2]. However, wings on UAV-sized scales have wing densities of a half-pound per square foot or less. Thus, there is a lot of potential wing weight savings if these configurations are used in the appropriate application. Nonetheless, these benefits must be weighed against their decreased aerodynamic efficiencies. The present research shows that some distributed lift configurations are able to generate up to 61% of the L/D of the mono-wing configuration. Keeping that in mind, the associated change in the Breguet range under a distributed lift configuration on various aircraft was investigated. It is important to note that this part of the study explores this performance metric exclusively, and not the stability and control implications which will be studied in a follow-up.

The three types of aircraft chosen were a Cessna 172, a Boeing F-18E, and a Boeing 747-100. Table 2 below shows these aircraft along with their max takeoff weights, true wing weights, and notional distributed lift configuration wing weights.

Table 2: Shows the Potential Weight Savings of Distributed Lift Configurations

Aircraft	MTOW (lbs)	Wing Weight (lbs)	Dist. Lift Wing Weight (lbs)	New Aircraft MTOW (lbs)	% Difference MTOW
Cessna 172	2,450	226	87	2,311	-6%
Boeing F-18E	47,000	4,799	250	42,451	-10%
Boeing 747-100	735,000	86,402	2,750	651,348	-12%

As the table shows, it can be noted that smaller aircraft such as a Cessna 172 don't experience as dramatic a weight savings, whereas something like the Boeing 747 is able to save more than 80,000 pounds in wing weight as a result of this configuration. The Breguet Range equation is shown below in Eq. 3:

$$Breguet\ Range = V * I_{sp} * \frac{L}{D} * \ln\left(\frac{W_i}{W_f}\right) \tag{3}$$

Two of the key terms in the Breguet Range equation are the L/D and the weights terms. For this study, the other two terms (V, I_{SP}) were held constant, so that the effect of varying the L/D and weights would have on the airplane's performance in terms of range could be observed. The L/D values varied from 45% all the way up to 100% in increments of 5%, although it is safe to state that a distributed lift configuration will never recover all of the aerodynamic efficiency of a mono-wing. The new weights were used in place of the old weights which also had some effect on the Breguet range. Figure 14 below shows these results for each of the three aircraft. Additionally, each aircraft's true range is plotted as a reference for each case. The plot clearly delineates the requisite weight savings to achieve parity with the conventional configuration. This ranges from roughly 85% for the 747-100 down to about 90% for the Cessna 172.

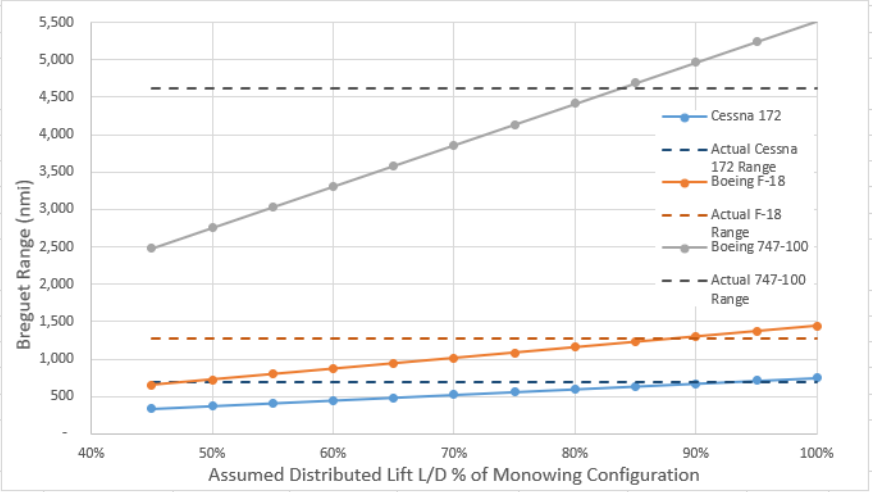

Figure 14. Shows Breguet Range Values Based on Changes in L/D and Aircraft Weight

VI. Conclusion

In building off of previous research on both bi-wing configurations and multi-wing distributed configurations, this research will look at the effects that decalage of wings in a multi-wing set have on the aerodynamic efficiency of the configuration. This began with a numerical test matrix rooted in the findings of the previous research on the placement of wings in a multi-wing configuration and proximity and placement of the wings with respect to one another both in vertical distance (gap) and top row stagger. These configurations underwent a VLM based numerical sensitivity on angle of attack of the wings downstream with both fixed and matched bottom row wing angles. Once the numerical testing is completed, an analysis on the results will provide the starting point for an experimental investigation that will validate the performance of the chosen sets and further validate the accuracy of the VLM code to predict performance of multi-wing configurations.

Conclusions of the experimental and numerical studies will be discussed here along with the analysis of the impacts of this study on the range of the three aircraft. Future considerations will also be discussed here. Comparisons will be made between the new findings from this study on decalage to the previous study with any major difference in performance being highlighted.

References

[1] Mongin, M., Truszkowski, A., Altman, A., *Aerodynamic Feasibility Study on Highly Distributed Lift Configurations Continued*, AIAA Region III Student Conference 2019

[2] Raymer, Daniel P. *Aircraft Design: A Conceptual Approach*, AIAA, 1992. doi: 10.2514/4.104909

[3] Kang, H., Genco, N., Altman, A., *Gap and Stagger Effects on Biplanes with End Plates Part I*, AIAA 09 -1085, 47th AIAA Aerospace Sciences Meeting and Exhibit, January 2009, Orlando, Florida. doi: 10.2514/6.2009-1085